

The stress and displacement fields at the tip of crazes in glassy polymers*

William E. Warren

Sandia National Laboratories, Albuquerque, New Mexico 87185, USA

(Received 1 November 1982; revised 25 February 1983)

This analysis models a craze region in glassy polymers as an elastic transversely isotropic homogeneous inclusion of thin elliptical shape with different elastic properties from the bulk polymer. The plane elasticity problem for an applied uniform stress field is solved and the results dimensionalized with respect to the craze tip radius. Stress and strain enhancements of several times far field values are found to occur at the craze tip and are independent of craze tip radius. These results are consistent with experimentally observed characteristics of craze growth and should be important in assessing the relative merits of different criteria that have been proposed for craze growth in glassy polymers.

Keywords Stress; crazes; fracture; plane elasticity; anisotropic elasticity; inclusion

INTRODUCTION

Crazes play an important role in the mechanical integrity of glassy polymers since they serve as precursors to the actual fracture of the polymer. As such, the phenomenon of crazing has received considerable theoretical and experimental attention over the years and summaries of the earlier work are contained in the survey articles of Rabinowitz and Beardmore¹ and Kambour². Broadly speaking, theoretical investigations of the mechanical properties of glassy polymers, including formation and growth of crazes, have proceeded along two rather distinct directions. The first, generally referred to as a kinetic theory, involves a micromolecular and thermodynamic approach in which the free energy of an element of the polymer is represented analytically and expressions for forces and pressures follow from differentiation of the free energy with respect to position or volume. Probabilistic representation of the entropy leads to Arrhenius type relations, refinements of this analysis being in more detailed statistical representations of the activation processes associated with the chain molecules to account for such effects as side chains, cross-linking, and chain scission. An excellent review of the kinetic theory is available in the book by Kausch³. One drawback to these kinetic theory analyses is that they are primarily scalar or one-dimensional, thus suppressing the tensorial nature of the stress and displacement fields. A second direction has been along the lines of a macroscopic or continuum mechanics approach in which the polymer is modelled as an elastic, viscoelastic, or plastic material. Reviews of this work are available in the survey papers of Knauss⁴ and Kramer⁵, and it is this second approach which is exploited in this work. An attempt to correlate and combine results from these two distinct approaches into a comprehensive theory of polymer fracture has been made by Andrews and Reed⁶.

Because of the importance of crazes in the eventual fracture of glassy polymers, a number of criteria for initiation and growth of crazes have been advanced. Within the framework of continuum mechanics, these have included critical stress criteria^{7,8}, critical strain criteria^{9,10}, energy release rate-fracture mechanics criteria^{11,12} and a dilatational stress criteria¹³. These criteria have been applied to the uniform loading conditions and not to the stress or strain conditions actually existing in a neighbourhood of the craze. This deficiency in the development of a criterion for craze initiation and growth has been recognized and several analyses of the stress field around a craze have been presented⁵. Following the original work of Knight¹⁴, all of these analyses have modelled the uncrazed polymer as a linear elastic body in plane stress or strain, and the craze region is modelled as a crack with either prescribed displacements representing the craze interface, or as an elastic foundation acting on the crack surface. Suppression of the inevitable stress singularity associated with the classical crack analysis by invoking a Dugdale-Barenblatt type annihilation results in stress and strain fields which provide very little enhancement at the craze tip, and craze tip shapes in the form of cusps which are considerably different from the blunted shapes observed experimentally.

To overcome the limitations associated with modelling the craze as a crack with elastic foundation properties, this analysis considers the craze region as an elastic transversely isotropic homogeneous inclusion of elliptical shape embedded in a second unbounded elastic isotropic material representing the bulk or uncrazed polymer. The bulk polymer is assumed to be in a condition of plane deformation and subjected to uniform loading conditions in the far field. Under these conditions, it is well known^{15,16} that the transversely isotropic elliptical inclusion is in a state of uniform stress. This fact, together with a straightforward application of the complex function theory of Muskhelishvili¹⁷ to the elastic isotropic region exterior to the elliptical inclusion, provides a closed-form solution to this plane elasticity problem. This

* This work performed at Sandia National Laboratories supported by the US Department of Energy under contract number DE-AC04-76DP00789.

solution is then represented as a power series in powers of the ratio of minor to major axis of the elliptical inclusion. For typical thin crazes, this ratio is very small and only the leading terms in this series representation are retained. With the help of a polar coordinate system with origin at a geometrical focus of the ellipse, the stress field in the neighbourhood of the craze tip is presented and discussed in detail. These results indicate that a bounded, very localized stress and strain enhancement of several times far field values is possible in the bulk polymer at the tip of the craze, and this enhancement is independent of the craze tip radius or craze length. Under these conditions, the shape of the craze tip remains blunted. The effect of this stress and strain enhancement at the craze tip on craze growth is yet to be determined but should be of interest in assessing the relative merits of different criteria that have been or may be proposed for craze growth in glassy polymers.

ELASTIC ANALYSIS

In this section we consider the plane elasticity problem of an elliptical shaped anisotropic homogeneous inclusion contained in an isotropic homogeneous matrix of infinite extent as shown in *Figure 1*. The isotropic elastic material exterior to the ellipse will be denoted as region 1, while the interior anisotropic elastic material will be denoted as region 2. Perfect bonding between these materials is assumed to occur at the elliptical interface, and the exterior region 1 is assumed subjected to a uniform stress state as infinity. Elliptical inclusion problems of this type have been the subject of numerous investigations over the years and of particular significance is the fact that under this condition of uniform loading in the far field, the inclusion is in a uniform stress state^{15,16}. This uniform stress condition is exploited in the analysis.

Analysis of region 1

The stress and displacement fields in the isotropic

elastic region 1 can be most readily obtained using the complex function theory of Muskhelishvili¹⁷. Accordingly, we represent the x - y plane as a complex z -plane, $z = x + iy$, and map this conformally into the exterior of the unit circle in a ζ -plane with the map

$$z = \omega(\zeta) = R(\zeta + 1/\zeta), \quad R > 0, \quad |\zeta| > 1. \quad (1)$$

The elliptical interior boundary of region 1 in the z -plane maps into a circle of radius $a > 1$ in the ζ -plane. The elliptical boundary has semi-minor axis m_1 and semi-major axis m_2 which are dependent on the parameter a such that

$$m_1 = R(a - 1/a), \quad m_2 = R(a + 1/a). \quad (2)$$

The appropriate complex potential functions $\phi(\zeta)$ and $\psi(\zeta)$ which provide a uniform stress field in the inclusion together with the prescribed stresses at infinity are

$$\begin{aligned} \phi(\zeta) &= \Gamma(\zeta + 1/\zeta) - a_{-1} \cdot \frac{1}{\zeta} \\ \psi(\zeta) &= \Gamma'(\zeta + 1/\zeta) + \frac{1}{(\zeta^2 - 1)}(b_{-1}\zeta + b_{-3}1/\zeta). \end{aligned}$$

In equation (3), Γ and Γ' are constants which relate to the uniform stress field at infinity and are given by

$$\begin{aligned} \Gamma &= \frac{R}{4}(\sigma_{x0} + \sigma_{y0}) \\ \Gamma' &= \frac{R}{2}(\sigma_{y0} - \sigma_{x0} + 2i\tau_0), \end{aligned} \quad (4)$$

where σ_{x0} , σ_{y0} , τ_0 designate the limit of σ_{xx} , σ_{yy} , σ_{xy} respectively as $z \rightarrow \infty$, and a_{-1} , b_{-1} , b_{-3} are constants to be determined from continuity of displacements and normal tractions at the elliptical interface. The stress and displacement fields in region 1 are represented in terms of

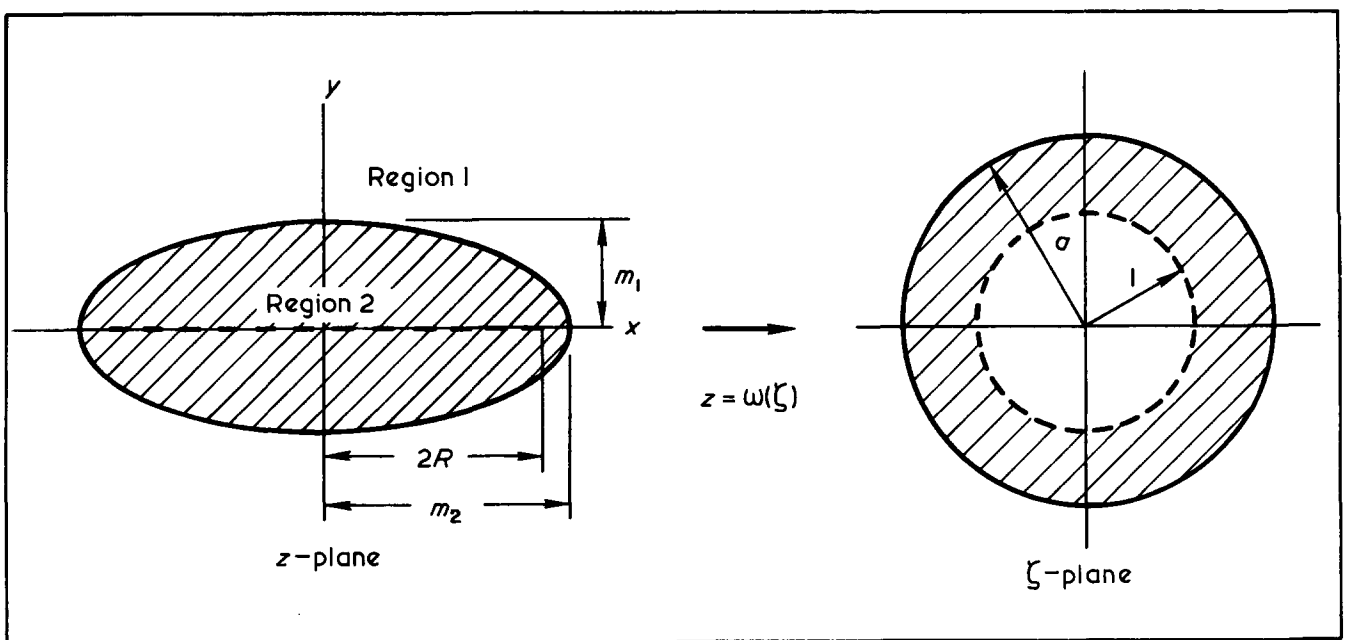


Figure 1 Geometry of plane elasticity elliptical inclusion problem

these potential functions, as

$$\begin{aligned}
 2G_1(u_1 + iv_1) &= \eta_1 \phi(\zeta) - \omega(\zeta) \overline{\Phi(\zeta)} - \overline{\psi(\zeta)} \\
 \sigma_{xx}^{(1)} + \sigma_{yy}^{(1)} &= 2[\Phi(\zeta) + \overline{\Phi(\zeta)}] \\
 \sigma_{yy}^{(1)} - \sigma_{xx}^{(1)} + 2i\sigma_{xy}^{(1)} &= 2 \left[\frac{\omega(\zeta)}{\omega'(\zeta)} \Phi'(\zeta) + \Psi(\zeta) \right], \quad (5)
 \end{aligned}$$

where u_1, v_1 are components of the displacement vector in the x and y directions respectively, G_1 is the shear modulus of the isotropic material of region 1, $\Phi(\zeta) = \phi'(\zeta)/\omega'(\zeta)$, $\Psi(\zeta) = \psi'(\zeta)/\omega'(\zeta)$, and

$$\eta_1 = \begin{cases} 3 - 4\nu_1 & \text{for plane strain} \\ \left(\frac{3 - \nu_1}{1 + \nu_1} \right) & \text{for plane stress,} \end{cases}$$

with ν_1 being Poisson's ratio for the material of region 1.

Analysis of region 2

The stress field in the anisotropic elliptical shaped inclusion of region 2 is known to be uniform^{15,16} so the stress and displacement fields can be immediately represented in terms of four constants, one of which represents a rigid body rotation of the inclusion. The general constitutive law for a transversely isotropic material requires five independent elastic constants, and for the y -axis being the axis of elastic symmetry, the stress-strain laws as provided by Eubanks and Sternberg¹⁸ take the form

$$\begin{aligned}
 \sigma_{xx} &= \alpha e_{xx} + b e_{yy} + (\alpha - 2\bar{\mu}) e_{zz} \\
 \sigma_{yy} &= b e_{xx} + \bar{\alpha} e_{yy} + b e_{zz} \\
 \sigma_{zz} &= (\alpha - 2\bar{\mu}) e_{xx} + b e_{yy} + \alpha e_{zz} \\
 \sigma_{xy} &= 2\mu e_{xy}, \quad \sigma_{yz} = 2\mu e_{yz}, \quad \sigma_{zx} = 2\bar{\mu} e_{zx}, \quad (6)
 \end{aligned}$$

where $e_{xx}, \dots, e_{xy}, \dots$ are the usual cartesian components of the strain tensor, and $\alpha, \bar{\alpha}, b, \mu, \bar{\mu}$ are the five independent elastic constants of which μ and $\bar{\mu}$ have an obvious physical meaning. Properties of these elastic constants are discussed in¹⁸ and also later in this paper. For a plane strain condition in the x - y plane, $e_{zz} = e_{zx} = e_{yz} = 0$ and equation (6) become

$$\begin{aligned}
 \sigma_{xx} &= \alpha e_{xx} + b e_{yy} \\
 \sigma_{yy} &= b e_{xx} + \bar{\alpha} e_{yy} \\
 \sigma_{xy} &= 2\mu e_{xy} \quad (7)
 \end{aligned}$$

with σ_{zz} depending linearly on σ_{xx} and σ_{yy} . A similar reduction occurs for conditions of generalized plane stress where $\sigma_{zz} = \sigma_{zx} = \sigma_{yz} = 0$, but these results will not be explicitly presented here.

Uniformity of the stress field of equation (7) in region 2 implies that the strains are constant and the associated displacements u_2, v_2 are linear functions of position. Thus in the complex ζ -plane we can represent the displacement

field in region 2 in the form

$$\begin{aligned}
 2\mu(u_2 + iv_2) &= (4C_1 + iC_4)(\zeta + 1/\zeta) \\
 &+ (4C_2 + iC_3)(\bar{\zeta} + 1/\bar{\zeta}) \quad (8)
 \end{aligned}$$

where C_1, C_2, C_3 and C_4 are real constants to be determined from the boundary conditions of region 1, C_4 representing a rigid body rotation of the elliptical inclusion. The usual complex stress combinations are

$$\begin{aligned}
 \sigma_{xx}^{(2)} + \sigma_{yy}^{(2)} &= 2 \left[\frac{(\alpha + \bar{\alpha} + 2b)}{\mu R} C_1 - \frac{(\bar{\alpha} - \alpha)}{\mu R} C_2 \right] \\
 \sigma_{yy}^{(2)} - \sigma_{xx}^{(2)} + 2i\sigma_{xy}^{(2)} &= 2 \left[\frac{(\bar{\alpha} - \alpha)}{\mu R} C_1 - \frac{(\alpha + \bar{\alpha} - 2b)}{\mu R} C_2 + i \frac{1}{R} C_3 \right]. \quad (9)
 \end{aligned}$$

Evaluation of constants

The seven constants $a_{-1}, b_{-1}, b_{-3}, C_1, C_2, C_3$ and C_4 are determined from the condition of continuity of displacements and normal stress at the interface between regions 1 and 2. In terms of the complex variable ζ , these continuity conditions take the form

$$\begin{aligned}
 u_1 + iv_1 &= u_2 + iv_2, \quad \text{on } \zeta = ae^{i\phi} \\
 \sigma_{\rho\rho}^{(1)} - i\sigma_{\rho\phi}^{(1)} &= \sigma_{\rho\rho}^{(2)} - i\sigma_{\rho\phi}^{(2)} \quad \text{on } \zeta = ae^{i\phi}, \quad (10)
 \end{aligned}$$

where $\sigma_{\rho\rho}$ and $\sigma_{\rho\theta}$ are the normal and tangential components of boundary stresses at the interface between regions 1 and 2. The conditions (10) provide a consistent set of equations for determining the seven constants, and evaluation provides

$$\begin{aligned}
 a_{-1} &= \frac{(a^4 - 1)}{2\mathcal{D}_2} \left\{ [4\Gamma + a^2(\Gamma' + \bar{\Gamma}')] \left[\left(1 + \frac{b}{G_1} \right) - \frac{(\alpha\bar{\alpha} - b^2)}{4G_1^2} \right] \right. \\
 &- \frac{\Gamma(\eta_1 + 1)}{2G_1} \left[(\bar{\alpha} - \alpha)a^2 + (\alpha + \bar{\alpha} + 2b) - \frac{(\alpha\bar{\alpha} - b^2)}{G_1} \right] \left. \right\} \\
 &- \frac{(a^4 - 1)}{2\mathcal{D}_1} (\Gamma' - \bar{\Gamma}') a^2 (1 - \mu/G_1) \\
 b_{-3} &= -\frac{(a^4 - 1)}{2\mathcal{D}_2} \left\{ (\Gamma' + \bar{\Gamma}') \left[\left(1 + \frac{b}{G_1} \right) - \frac{(\alpha\bar{\alpha} - b^2)}{4G_1^2} \right] (a^4 - 1) \right. \\
 &+ [(\Gamma' + \bar{\Gamma}') - 4a^2\Gamma] \frac{(\eta_1 + 1)}{4G_1} \left[(\bar{\alpha} - \alpha)a^2 + (\alpha + \bar{\alpha} + 2b) \right. \\
 &\quad \left. \left. - \frac{(\alpha\bar{\alpha} - b^2)}{G_1} \right] \right\} \\
 &+ \frac{\Gamma(\eta_1 + 1)}{2G_1} \left[(\bar{\alpha} - \alpha)(a^4 - 1) + 8ba^2 + (\eta_1 - 3) \frac{(\alpha\bar{\alpha} - b^2)}{G_1} a^2 \right] \left. \right\} \\
 &+ \frac{(a^4 - 1)}{2\mathcal{D}_1} (\Gamma' - \bar{\Gamma}') (1 - \mu/G_1) (a^4 + 1)
 \end{aligned}$$

$$\begin{aligned}
 C_1 &= \frac{\mu(\eta_1 + 1)}{16G_1\mathcal{D}_2} \left\{ [2\Gamma + a^2(\Gamma' + \bar{\Gamma}')] \left[2 - \frac{(\bar{\alpha} - b)}{2G_1} (a^2 + 1) \right. \right. \\
 &\quad \left. \left. + \frac{(\alpha - b)}{2G_1} (a^2 - 1) \right] \right. \\
 &\quad \left. + 2a^2\Gamma \left[2a^2 + \eta_1 \frac{(\bar{\alpha} - b)}{2G_1} (a^2 + 1) \right. \right. \\
 &\quad \left. \left. + \eta_1 \frac{(\alpha - b)}{2G_1} (a^2 - 1) \right] \right\} \\
 C_2 &= -\frac{\mu(\eta_1 + 1)}{16G_1\mathcal{D}_2} \left\{ [2\Gamma + a^2(\Gamma' + \bar{\Gamma}')] \left[2a^2 + \frac{(\bar{\alpha} + b)}{2G_1} (a^2 + 1) \right. \right. \\
 &\quad \left. \left. + \frac{(\alpha + b)}{2G_1} (a^2 - 1) \right] \right. \\
 &\quad \left. + 2a^2\Gamma \left[2 - \eta_1 \frac{(\bar{\alpha} + b)}{2G_1} (a^2 + 1) + \eta_1 \frac{(\alpha + b)}{2G_1} (a^2 - 1) \right] \right\} \\
 C_3 &= \frac{\mu(\eta_1 + 1)}{2iG_1\mathcal{D}_1} (\Gamma' - \bar{\Gamma}') a^4 \\
 C_4 &= -\frac{\mu(\eta_1 + 1)}{2iG_1\mathcal{D}_1} (\Gamma' - \bar{\Gamma}') (1 - \mu/G_1) a^2 \\
 b_{-1} &= -b_{-3} - \frac{(a^4 + 1)}{a^2} a_{-1} \quad (11)
 \end{aligned}$$

where

$$\begin{aligned}
 \mathcal{D}_1 &= \left(1 + \frac{\mu}{G_1} \eta_1 \right) a^4 - (1 - \mu/G_1), \\
 \mathcal{D}_2 &= \frac{(\eta_1 + 1)}{4G_1} [\alpha(a^2 - 1)^2 + \bar{\alpha}(a^2 + 1)^2] \\
 &\quad + \left[1 - (\eta_1 - 1) \frac{b}{2G_1} + \eta_1 \frac{(\alpha\bar{\alpha} - b^2)}{4G_1^2} \right] (a^4 - 1) \quad (12)
 \end{aligned}$$

This completes the analysis of the plane elasticity problem, the stress and displacement fields in both regions being obtainable from equations (5), (8) and (9). Consideration is now directed to a limiting form of the solution as the ellipse becomes very thin.

STRESS FIELD AT A CRAZE TIP

In this section we utilize the results obtained from the elastic analysis together with the geometric properties of typical crazes to obtain relatively simple expressions for the stress and displacement fields both in the craze itself and in the bulk polymer in a neighbourhood of the craze tip. Physical observations of crazes show them to be very long and thin, a characteristic which has led to their being modelled as cracks rather than elastic inclusions in previous theoretical treatments. In the present analysis, we interpret this condition as providing an elliptical

inclusion in which the ratio of minor to major axis is very small. Accordingly, we define the parameter ϵ as the ratio of minor to major axis of the elliptical inclusion, equation (2) giving

$$\epsilon = \frac{m_1}{m_2} = \frac{(a^2 - 1)}{(a^2 + 1)} \ll 1, \quad (13)$$

and relate all the geometrical properties of the inclusion to the parameter ϵ .

The complex stress combinations in the bulk polymer of region 1 are obtained from equations (3) and (5) and may be put in the form

$$\begin{aligned}
 \sigma_{xx}^{(1)} + \sigma_{yy}^{(1)} &= \frac{2}{R} \left\{ 2\Gamma + \frac{a_{-1}}{(a^4 - 1)} \cdot \frac{(a^4 - 1)}{(\zeta^2 - 1)} + \frac{\bar{a}_{-1}}{(a^4 - 1)} \cdot \frac{(a^4 - 1)}{(\bar{\zeta}^2 - 1)} \right\} \\
 \sigma_{yy}^{(1)} - \sigma_{xx}^{(1)} + 2i\sigma_{xy}^{(1)} &= \frac{2}{R} \left\{ \Gamma' + 2 \frac{a_{-1}}{(a^4 - 1)} \cdot \frac{\zeta^2(\zeta - \bar{\zeta})(\zeta\bar{\zeta} - 1)(a^4 - 1)}{\bar{\zeta}(\zeta^2 - 1)^3} \right. \\
 &\quad \left. + \frac{a_{-1}}{(a^4 - 1)} \cdot \frac{(a^2 + 1)}{a^2} \left[2 \frac{(a^2 - 1)^3}{(\zeta^2 - 1)^3} + 3 \frac{(a^2 - 1)^3}{(\zeta^2 - 1)^2} \right] \right. \\
 &\quad \left. + \left[\frac{b_{-3}}{(a^4 - 1)} + \frac{a_{-1}}{(a^4 - 1)} \cdot \frac{(a^2 - 1)^2}{a^2} \right] \frac{(a^4 - 1)}{(\zeta^2 - 1)} \right\}. \quad (14)
 \end{aligned}$$

To investigate the nature of this stress field in a neighbourhood of the craze tip, we now define a polar coordinate system (r, θ) with origin at the right focus $z = 2R$ as shown in Figure 2. Thus

$$z = 2R + re^{i\theta} = R(\zeta + 1/\zeta)$$

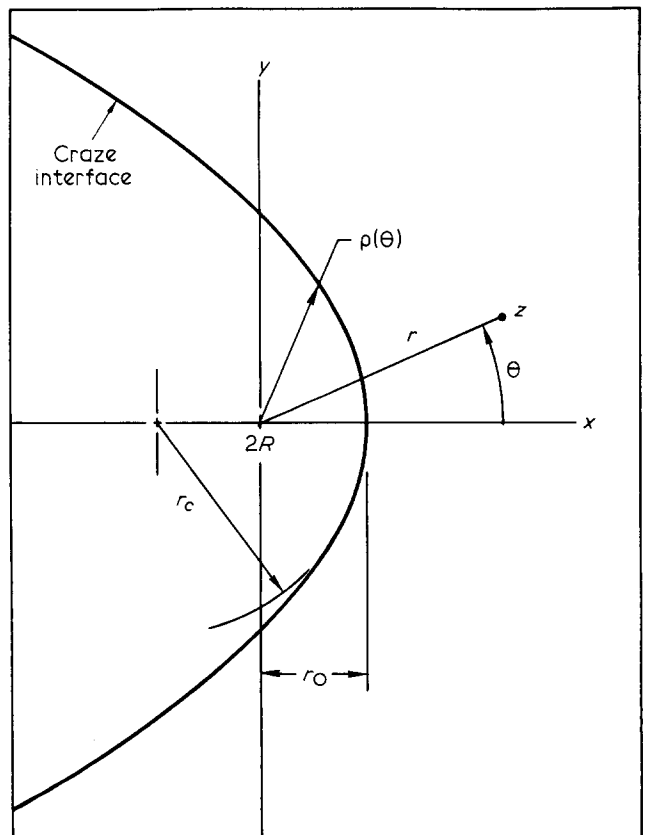


Figure 2 Geometry of craze tip

which may be inverted to provide

$$\zeta = 1 + \frac{1}{2} \frac{r}{R} e^{i\theta} + \sqrt{\frac{r}{R} e^{i\theta/2}} \sqrt{1 + \frac{1}{4} \frac{r}{R} e^{i\theta}}. \quad (15)$$

The minimum distance from the focus to the craze boundary, r_0 as shown in Figure 2, is

$$r_0/R = \frac{(a-1)^2}{a} = \varepsilon^2(1\frac{3}{4}\varepsilon^2 + \dots), \quad (16)$$

while the radius of curvature r_c at the tip of the craze is

$$r_c/R = \frac{(a^2-1)^2}{a(a^2+1)} = 2\varepsilon^2(1 + \frac{1}{2}\varepsilon^2 + \dots). \quad (17)$$

The equation of the elliptical craze interface occurring at $r = \rho(\theta)$ is

$$\frac{\rho(\theta)}{r_0} = \frac{(a+1)^2}{[(a^2+1) + 2a \cos \theta]} \\ = [\cos^2 \theta/2]^{-1} \left[1 - \frac{1}{4}\varepsilon^2 \frac{(1-\cos \theta)}{(1+\cos \theta)} + \dots \right]. \quad (18)$$

From equations (15) and (16) we arrive at the important result

$$\frac{(a^2-1)}{(\zeta^2-1)} = \sqrt{\frac{r_0}{r}} e^{-i\theta/2} \left[1 + \varepsilon \left(1 - \sqrt{\frac{r}{r_0}} e^{i\theta/2} \right) + \dots \right], \quad (19)$$

and since $r \gg \rho \geq r_0$ in region 1, this quantity remains bounded for all r, θ in region 1. Expanding the coefficients a_{-1} and b_{-3} of equation (11) in powers of ε and retaining only the leading term provides

$$\frac{a_{-1}}{(a^4-1)} = \frac{R}{4} (\sigma_{x0} M_x + \sigma_{y0} M_y - i\tau_0 M_{xy}) \\ \frac{b_{-3}}{(a^4-1)} = \frac{R}{4} (\sigma_{x0} N_x + \sigma_{y0} N_y + i\tau_0 N_{xy}), \quad (20)$$

where

$$M_x = \frac{1}{4\bar{\alpha}} \left[\frac{(\alpha\bar{\alpha} - b^2)}{G_1} - 2(\bar{\alpha} + b) \right] \\ M_y = \frac{4G_1}{\bar{\alpha}(\eta_1 + 1)} \left[1 + \frac{b}{G_1} - \frac{(\bar{\alpha} + b)}{8G_1} (\eta_1 + 1) \right. \\ \left. + \frac{(\alpha\bar{\alpha} - b^2)}{16G_1^2} (\eta_1 - 3) \right] \\ N_x = \frac{1}{\bar{\alpha}} \left[2\bar{\alpha} - \frac{(\alpha\bar{\alpha} - b^2)}{4G_1} (\eta_1 + 1) \right] \\ N_y = \frac{1}{\alpha} \left[2b + \frac{(\alpha\bar{\alpha} - b^2)}{4G_1} (\eta_1 - 3) \right] \\ N_{xy} = 2M_{xy} = \frac{8G_1}{\mu(\eta_1 + 1)} (1 - \mu/G_1), \quad (21)$$

and the complex stress combinations of equation (14) become

$$\sigma_{xx}^{(1)} + \sigma_{yy}^{(1)} = (\sigma_{x0} + \sigma_{y0}) - 2\tau_0 M_{xy} \sqrt{\frac{r_0}{r}} \sin \theta/2 \\ + 2(\sigma_{x0} M_x + \sigma_{y0} M_y) \sqrt{\frac{r_0}{r}} \cos \theta/2 \quad (22)$$

and

$$\sigma_{yy}^{(1)} - \sigma_{xx}^{(1)} + 2i\sigma_{xy}^{(1)} = (\sigma_{y0} - \sigma_{x0} + 2i\tau_0) \\ + (\sigma_{x0} M_x + \sigma_{y0} M_y - i\tau_0 M_{xy}) \sqrt{\frac{r_0}{r}} e^{-i3\theta/2} \left[2\left(\frac{r_0}{r}\right) + i \sin \theta \right] \\ + (\sigma_{x0} N_x + \sigma_{y0} N_y + i\tau_0 N_{xy}) \sqrt{\frac{r_0}{r}} e^{-i\theta/2}. \quad (23)$$

In the results (22) and (23), terms of order ε have been suppressed. The associated strain fields may be readily obtained from equations (22) and (23) using

$$e_{xx}^{(1)} + e_{yy}^{(1)} = \frac{(\eta_1 - 1)}{4G_1} (\sigma_{xx}^{(1)} + \sigma_{yy}^{(1)}) \\ e_{yy}^{(1)} - e_{xx}^{(1)} + 2ie_{xy}^{(1)} = \frac{1}{2G_1} (\sigma_{yy}^{(1)} - \sigma_{xx}^{(1)} + 2i\sigma_{xy}^{(1)}) \quad (24)$$

which are important relations for considering certain strain induced craze growth criteria^{9,10}. We note that the craze tip stress fields of equations (22) and (23) remain bounded for all r_0 , and in fact the stress at the craze interface is independent of r_0 as can be readily shown by letting $r \rightarrow \rho$, a boundary point, and using equation (18). The complex stress combinations at the boundary become

$$[\sigma_{xx}^{(1)} + \sigma_{yy}^{(1)}]_b = (\sigma_{x0} + \sigma_{y0}) - \tau_0 M_{xy} \sin \theta \\ + (\sigma_{x0} M_x + \sigma_{y0} M_y)(1 + \cos \theta) \\ [\sigma_{yy}^{(1)} - \sigma_{xx}^{(1)} + 2i\sigma_{xy}^{(1)}]_b = (\sigma_{y0} - \sigma_{x0} + 2i\tau_0) - \tau_0 M_{xy} \sin \theta e^{-i\theta} \\ + (\sigma_{x0} M_x + \sigma_{y0} M_y)(1 + \cos \theta) e^{-i\theta} \\ + \frac{1}{2}(\sigma_{x0} N_x + \sigma_{y0} N_y)(1 + e^{-i\theta}) \quad (25)$$

The amplitude of the complex stress combination (25₂) is equal to 2τ , where τ is the maximum shear stress at a boundary point. A direct evaluation reveals that this shear stress and also the normal stress combination (25₁) exhibit their maximum values at the same point on the boundary for any combination of applied loads if the relations

$$M_{xy}(N_y + N_x) = 4(M_y + M_x) \\ M_{xy}(4 + N_y - N_x) = 4(M_y - M_x) \\ \text{hold. These two relations are satisfied if} \\ \alpha = \bar{\alpha}, \quad 2\mu = \bar{\alpha} - b. \quad (26)$$

That is, if the material constants of the craze satisfy the

additional conditions of equation (26), then the point of maximum shear stress on the craze boundary in region 1 occurs at the same point as the point of maximum hydrostatic stress on the boundary. This restriction on the elastic constants of the craze will be discussed later but we mention here that the conditions of equation (26) are satisfied if the craze is isotropic rather than transversely isotropic. More important, the effect of this condition when the maximum shear stress and the maximum hydrostatic stress occur at the same point on the boundary is that all the other variables which have been postulated to cause craze growth also maximize at this same point. Thus the maximum principal stress, maximum principal strain, maximum shear stress, maximum shear strain, along with the usual linear combinations of these quantities to represent, for example, Mohr-Coulomb yielding, all occur at the same point in the bulk polymer at the craze boundary. If the craze does actually behave mechanically so that this occurs, the effect would appear to make all of the postulated craze growth criteria essentially identical and mask the actual effect responsible for craze growth. This may in part account for the numerous craze growth theories advanced over the years and for the lack of general acceptance of any of these theories.

Within the crazed region the stresses are uniform, and while the craze itself is not a continuous elastic material, these effective stresses may be of interest in investigating the eventual fracture of the craze. Suppressing terms of order ε in equation (9), this uniform stress field becomes

$$\sigma_{xx}^{(2)} = \frac{b}{\alpha} \sigma_{y0} + [(\eta_1 + 1)\sigma_{x0} + (\eta_1 - 3)\sigma_{y0}] \frac{(\alpha\bar{x} - b^2)}{8\bar{\alpha}G_1}$$

$$\sigma_{yy}^{(2)} = \sigma_{y0}, \quad \sigma_{xy}^{(2)} = \tau_0. \quad (27)$$

The rigid body angular rotation Ω of the craze, positive Ω being counter-clockwise, is given by

$$\Omega = \frac{1}{2} \left(\frac{\partial v_2}{\partial x} - \frac{\partial u_2}{\partial y} \right) = \frac{1}{2\mu R} C_4$$

and suppressing terms of order ε , this becomes

$$\Omega = -\frac{\tau_0}{2\mu} (1 - \mu/G_1) \quad (28)$$

The displacement field at the craze tip can be represented as the sum of the displacement of the focus plus a relative displacement of the craze with respect to the focus. Thus at the right hand craze tip we again take $z = 2R + re^{i\theta}$ in equation (8) to get

$$u_2 + iv_2 = (U_2 + iV_2) + (u_2 + iv_2)_{rel}. \quad (29)$$

where $(U_2 + iV_2)$ is the displacement of the right focus point given by

$$U_2 + iV_2 = \frac{R}{4G_1} [(\eta_1 + 1)\sigma_{x0} + (\eta_1 - 3)\sigma_{y0} + 4i\tau_0] \quad (30)$$

where terms of order ε have been suppressed. The relative displacement is

$$(u_2 + iv_2)_{rel} = \frac{r}{2G_1} \left\{ \frac{1}{4} [(\eta_1 + 1)\sigma_{x0} + (\eta_1 - 3)\sigma_{y0}] \cos \theta \right. \\ \left. + \tau_0 \frac{G_1}{\mu} \left(2 - \frac{\mu}{G_1} \right) \sin \theta \right\} \\ + i \left\{ 2 \frac{G_1}{\alpha} \sigma_{y0} \sin \theta + \tau_0 \cos \theta \right. \\ \left. - \frac{1}{4} \frac{b}{\alpha} [(\eta_1 + 1)\sigma_{x0} + (\eta_1 - 3)\sigma_{y0}] \sin \theta \right\} \quad (31)$$

for

$$r \leq \rho(\theta) = r_0 [\cos^2 \theta / 2]^{-1} = \varepsilon^2 R [\cos^2 \theta / 2]^{-1},$$

and we note that this relative displacement is of order ε^2 compared with the displacement of the focus. The radius of curvature at the tip of the craze remains effectively undeformed and the craze tip remains blunted.

ELASTIC CONSTANTS

Because of the importance of the elastic constants in defining the magnitude of the stress field at the tip of a craze as determined from this analysis, we now provide a discussion of these constants. The material of the exterior region, region 1, is the uncrazed bulk polymer and is assumed to be a linear isotropic elastic solid. Thus the mechanical properties of region 1 are completely defined in terms of two elastic constants taken here to be the shear modulus G_1 and Poisson's ratio ν_1 . The physical interpretation of these two constants, or equivalently the material Young's modulus E_1 , bulk modulus k_1 , or the Lamé constant λ_1 is well understood and experimentally measured values of these constants are available in the literature for most polymers. The obvious temperature dependence of these constants, though not explicitly acknowledged, is assumed.

The material in the elliptical shaped interior region, region 2, models the crazed polymer and this is represented as a transversely isotropic homogeneous elastic solid with axis of elastic symmetry normal to the plane of the craze. Physical observations of craze regions indicate them to be rather complex structures including intermittent void regions with load bearing ligaments running primarily normal to the craze plane. As such, the craze region is clearly not a continuous elastic material, and modelling the craze as such requires an interpretation of the elastic constants in terms of the effective mechanical properties. Also, the density of voids in the craze region appears to be nonuniform, decreasing near the craze tip, but neither this nor any other possible nonhomogeneous mechanical effects within the craze are considered. Since there appears to be no preferred orientation of the craze with respect to the plane of the craze in polymers which are otherwise isotropic, the assumption of transverse isotropy would appear to be quite realistic. It is also likely that the mechanical properties of the craze and hence the elastic constants associated with this model of the craze are also temperature dependent but this is not explicitly represented.

Transversely isotropic elastic materials are characterized by five independent elastic constants, one set of which have already been defined in the stress-strain relations of equation (6). A more useful physical interpretation of these constants can be obtained by inverting equation (6) and writing them in the form

$$\begin{aligned} e_{xx} &= \frac{1}{E} [\sigma_{xx} - \nu\sigma_{zz} - \bar{\nu}\sigma_{yy}] \\ e_{yy} &= \frac{1}{\bar{E}} \left[\sigma_{yy} - \frac{\bar{\nu}\bar{E}}{E} (\sigma_{xx} + \sigma_{zz}) \right] \\ e_{zz} &= \frac{1}{E} [\sigma_{zz} - \nu\sigma_{xx} - \bar{\nu}\sigma_{yy}] \\ e_{xy} &= \frac{\sigma_{xy}}{2\mu}, \quad e_{yz} = \frac{\sigma_{yz}}{2\mu}, \quad e_{xz} = \frac{\sigma_{xz}}{2\bar{\mu}} \end{aligned} \quad (32)$$

From equation (32) we observe that E is the effective Young's modulus of the craze taken in any direction lying in the plane of the craze, \bar{E} is the effective Young's modulus of the craze in a direction normal to the plane of the craze, while ν and $\bar{\nu}$ represent effective Poisson's ratios coupling strain in the plane of the craze with stresses applied normal to the direction of strain in the craze plane and normal to the craze plane respectively. The constants μ and $\bar{\mu}$ represent the effective shear moduli for shearing stresses applied out of the craze plane and within the craze plane respectively. The relations connecting the elastic constants of equation (32) with those of equation (6) are

$$\begin{aligned} E &= \frac{4\bar{\mu}(\alpha\bar{\alpha} - b^2 - \bar{\alpha}\bar{\mu})}{(\alpha\bar{\alpha} - b^2)}, \quad \bar{E} = \frac{(\alpha\bar{\alpha} - b^2 - \bar{\alpha}\bar{\mu})}{(\alpha - \bar{\mu})} \\ \nu &= \frac{(\alpha\bar{\alpha} - b^2 - 2\bar{\alpha}\bar{\mu})}{(\alpha\bar{\alpha} - b^2)}, \quad \bar{\nu} = \frac{2b\bar{\mu}}{(\alpha\bar{\alpha} - b^2)} \end{aligned} \quad (33)$$

with inverse

$$\begin{aligned} \alpha &= \frac{E(E - \bar{\nu}^2\bar{E})}{(1 + \nu)[(1 - \nu)E - 2\bar{\nu}^2\bar{E}]}, \quad b = \frac{\bar{\nu}\bar{E}}{[(1 - \nu)E - 2\bar{\nu}^2\bar{E}]} \\ \bar{\alpha} &= \frac{(1 - \nu)E\bar{E}}{[(1 - \nu)E - 2\bar{\nu}^2\bar{E}]}, \quad \bar{\mu} = \frac{E}{2(1 + \nu)} \end{aligned} \quad (34)$$

We note that the shear modulus μ is independent of the other defined elastic constants. To insure positive definiteness of the strain energy function for the craze material, Eubanks and Sternberg¹⁸ have shown that the following inequalities must be satisfied:

$$\begin{aligned} \alpha > 0, \quad \bar{\alpha} > 0, \quad \mu > 0, \quad \bar{\mu} > 0, \\ (\alpha\bar{\alpha} - b^2 - \bar{\alpha}\bar{\mu}) > 0, \end{aligned} \quad (35a)$$

or equivalently

$$\begin{aligned} E > 0, \quad \bar{E} > 0, \quad \mu > 0, \quad \bar{\mu} > 0, \\ -1 < \nu < 1, \quad 1 - \nu > 2\frac{\bar{E}}{E}\bar{\nu}^2. \end{aligned} \quad (35b)$$

The nature of crazed regions in polymers makes it unlikely that these material constants can be obtained by

direct measurement and hence numerical values for these constants must be inferred from observations and from indirect measurements made on the composite system of bulk polymer and craze. For example, the nature of the extensive void region in the craze and the load carrying ligaments aligned transverse to the plane of the craze would indicate that a stress σ_{yy} applied normal to the craze plane would induce very little strain e_{xx} or e_{zz} within the craze plane, and a realistic assumption might be that the effective Poisson's ratio $\bar{\nu} = 0$. Also, comparative measurements of the transverse strain in the central region of the craze and in the bulk polymer under conditions of uniaxial loading normal to the craze plane should provide the ratio of \bar{E} to the Young's modulus of the bulk polymer. Results presented by Kambour² indicate this ratio to be somewhere between 1/3 to 1/4 for some typical polymer materials. Determination of the remaining three elastic constants E , ν , and μ will require additional information and probably additional assumptions about the nature of the craze material itself. It would appear quite probable that $E < \bar{E}$ but such an assumption would need experimental verification.

It is possible that all the mechanical effects in the bulk polymer exhibit their maximum values at the same point on the craze boundary and that the elastic constants of the craze satisfy the two additional conditions defined in equation (26). If this is true, the five independent elastic constants of the craze region are reduced to three which could be taken, for example, as $(E, \bar{E}, \bar{\nu})$ or $(E, \nu, \bar{\nu})$. The reduction of the elastic constants from five to three implied by equation (26) does not result in any of the three constant cubic crystal classes as originally developed by Voigt¹⁹ and discussed by Love²⁰. Assuming the craze region to be completely isotropic further reduces the elastic constants to two. Experimental verification of these reductions does not appear to be available. Because of lack of information about these elastic constants, we assume in the numerical example of the next section that the craze region is isotropic and thus characterized by two independent elastic constants.

NUMERICAL EXAMPLE

We now consider a specific example of the previous analysis and show how the stress field varies around the tip of the craze. Because of uncertainties about the values of the five elastic constants associated with the transversely isotropic craze material we assume for this example that the craze is isotropic and its mechanical properties characterized by two elastic constants which are taken as the shear modulus G_2 and Poisson's ratio ν_2 . Major interest here is on the nature of the stress field in the isotropic bulk polymer in a neighbourhood of the craze tip, and while the assumption of isotropy of the craze may effect these numerical results quantitatively by providing different values for the constants M_x, \dots, N_x, \dots , the qualitative results should be retained. Also, taking Poisson's ratio $\nu_2 = 0$ effectively uncouples transverse strains from axial stresses which appears to be a characteristic of the craze. For the isotropic craze the elastic constants reduce to

$$\begin{aligned} \alpha = \bar{\alpha} &= \frac{2(1 - \nu_2)G_2}{(1 - 2\nu_2)}, \quad b = \frac{2\nu_2G_2}{(1 - 2\nu_2)} \\ \mu = \bar{\mu} &= G_2 \end{aligned} \quad (36)$$

which also satisfy the conditions of equation (26). For this example we will take

$$G_1/G_2 = 4, \quad \nu_1 = 0.348, \quad \nu_2 = 0 \quad (37)$$

which gives a ratio of Young's modulus for the craze to the bulk polymer of about 1/5. The constants of equation (21) become

$$\begin{aligned} M_x &= -0.375 & N_x &= 1.674 \\ M_y &= 2.50 & N_y &= 0.174 \\ M_{xy} &= 4.60 & N_{xy} &= 9.20. \end{aligned} \quad (38)$$

For this example the uniform stress field at infinity will be taken as a uniaxial stress of magnitude σ_0 with direction γ measured clockwise from the y -axis. This results in the uniform stress condition

$$\begin{aligned} \sigma_{x0} &= \sigma_0 \sin^2 \gamma \\ \sigma_{y0} &= \sigma_0 \cos^2 \gamma \\ \tau_{0} &= \sigma_0 \sin \gamma \cos \gamma \end{aligned} \quad (39)$$

Using equations (38) and (39) in equations (22) and (23) gives the stress field in the bulk polymer in a neighbourhood of the craze tip under conditions of plane strain. Figure 3 shows the contour lines of constant hydrostatic stress S defined by

$$S = \frac{1}{3}(\sigma_{xx}^{(1)} + \sigma_{yy}^{(1)} + \sigma_{zz}^{(1)}) = \frac{1}{3}(1 + \nu_1)(\sigma_{xx}^{(1)} + \sigma_{yy}^{(1)}) \quad (40)$$

for $\gamma = 0$, that is, for the applied stress directed normal to the plane of the craze. The maximum value occurs at the craze tip $r = r_0, \theta = 0$ and provides a stress enhancement of $S/S_\infty = 6$ at this point. The uniform hydrostatic stress field within the craze as obtained from equation (27) is $(S/S_\infty)_{\text{craze}} = 0.68$. The effect of this stress field S would be to propagate the craze along the x -axis, $\theta = 0$, which is consistent with numerous observations indicating that craze growth occurs in a direction perpendicular to the direction of applied stress. Figure 4 shows the contour lines of constant maximum shear stress τ defined by

$$\begin{aligned} \tau &= \frac{1}{2}[(\sigma_{yy}^{(1)} - \sigma_{xx}^{(1)})^2 + 4\sigma_{xy}^{(1)2}]^{1/2} \\ &= \frac{1}{2}\{(\sigma_{yy}^{(1)} - \sigma_{xx}^{(1)} + 2i\sigma_{xy}^{(1)})(\sigma_{yy}^{(1)} - \sigma_{xx}^{(1)} - 2i\sigma_{xy}^{(1)})\}^{1/2} \end{aligned} \quad (41)$$

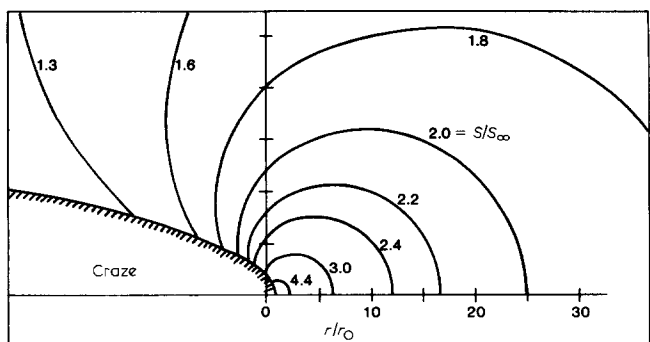


Figure 3 Contour lines of constant hydrostatic stress, S/S_∞ , at craze tip for a uniaxial load directed normal to the craze plane, $\gamma = 0^\circ$

for the same case where the externally applied stress is directed normal to the craze plane, $\gamma = 0$. The maximum value of τ also occurs at $r = r_0, \theta = 0$ and a shear stress enhancement of $\tau/\tau_\infty = 6.17$ occurs at this point. Within the craze, $(\tau/\tau_\infty)_{\text{craze}} = 1.08$. The enhancement of S and τ for this situation are almost identical. The shear stress enhancement of Figure 4 is considerably more localized than the hydrostatic stress enhancement of Figure 3 and it is not clear that the effect of the shear stress is to propagate the craze along the x -axis. Other possible effects could be the generation of shear bands skewed at some angle from the x -axis which have been observed experimentally by Newman and Wolock²¹, or bifurcation of the craze plane which has apparently not been observed.

Figures 5 and 6 show contour lines of hydrostatic stress S and maximum shear stress τ when the applied uniaxial stress σ_0 has direction $\gamma = 45^\circ$ and we observe that these contour lines are considerably skewed from those of the

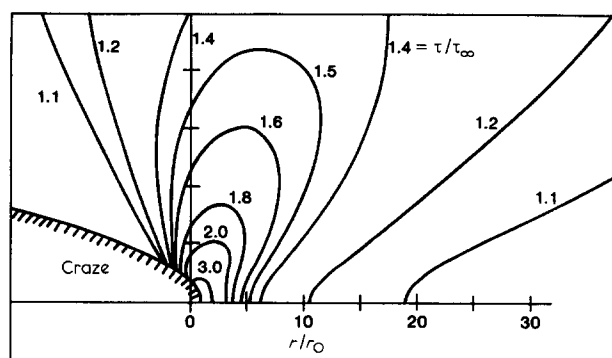


Figure 4 Contour lines of constant maximum shear stress, τ/τ_∞ , at craze tip for a uniaxial load directed normal to the craze plane, $\gamma = 0^\circ$

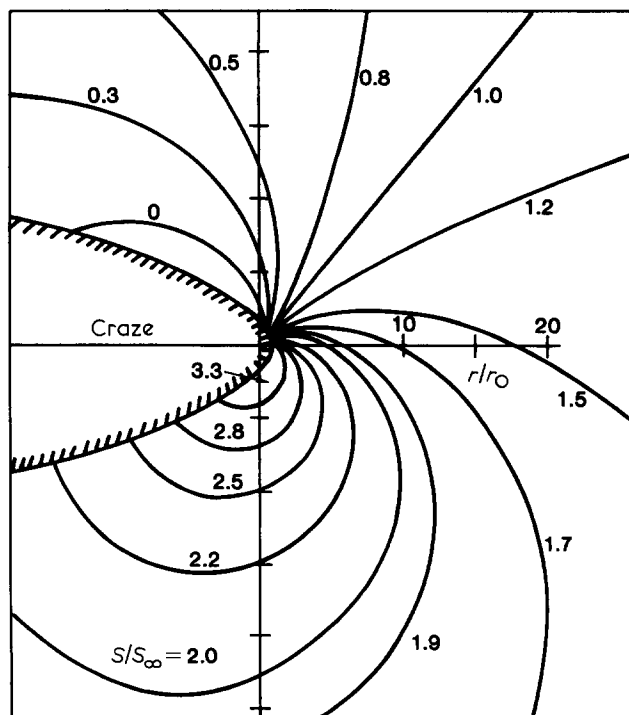


Figure 5 Contour lines of constant hydrostatic stress, S/S_∞ , at craze tip for a uniaxial load directed 45° from the craze plane normal, $\gamma = 45^\circ$

previous example. The maximum enhancement of S and τ occurs at the craze boundary at an angle $\theta = -65^\circ$ and the enhancements at this point are $S/S_\infty = 4.59$ and $\tau/\tau_\infty = 5.16$. For this condition, the shear stress enhancement is 12% greater than the hydrostatic stress enhancement although both are less than the enhancement of the previous example where the applied stress was directed normal to the craze plane. It would appear that the effect of this stress field around the craze tip would be to deflect the growth of the craze toward a direction more closely perpendicular to the direction of applied stress. This effect of curving craze growth has been observed experimentally in polystyrene films by King and Kramer²² under loading conditions of varying biaxial stress. The uniform stress field in the craze provides the values $(S/S_\infty)_{\text{craze}} = 0.49$ and $(\tau/\tau_\infty)_{\text{craze}} = 1.10$ so the shear effect for this direction of loading is quite evident in the crazed region. The rigid body rotation of the craze is $\Omega = -0.75 \sigma_0/G_1$ which tends toward lining up the craze perpendicular to the direction of applied stress.

Figures 7 and 8 show conour lines of constant S and τ for the case where the uniaxial stress σ_0 is applied in a direction parallel to the craze plane, $\gamma = 90^\circ$. For this direction of applied stress, the effect of the craze is to decrease the stress at the craze tip and effectively suppress craze growth at this point, a much observed physical effect in crazed polymers. At the craze tip $r = r_0$, $\theta = 0$, the hydrostatic stress is $S/S_\infty = 0.24$, and the shear stress is $\tau/\tau_\infty = 0$. A line of zero shear stress extends out from the craze tip about one craze tip radius. The uniform stress field in the craze region has values $(S/S_\infty)_{\text{craze}} = 0.12$ and $(\tau/\tau_\infty)_{\text{craze}} = 0.16$.

Figure 9 shows how the two stress combinations S/S_∞ and τ/τ_∞ in the bulk polymer vary around the craze boundary for the three directions of externally applied uniaxial stress just considered. Table 1 provides a listing of the maximum enhancement of several variables which

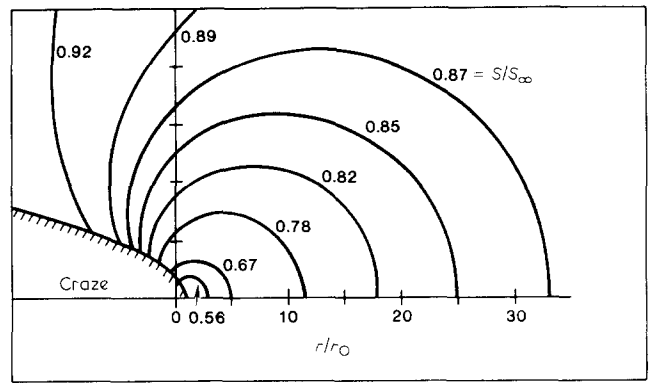


Figure 7 Contour lines of constant hydrostatic stress, S/S_∞ , at craze tip for a uniaxial load directed parallel to the craze plane, $\gamma = 90^\circ$

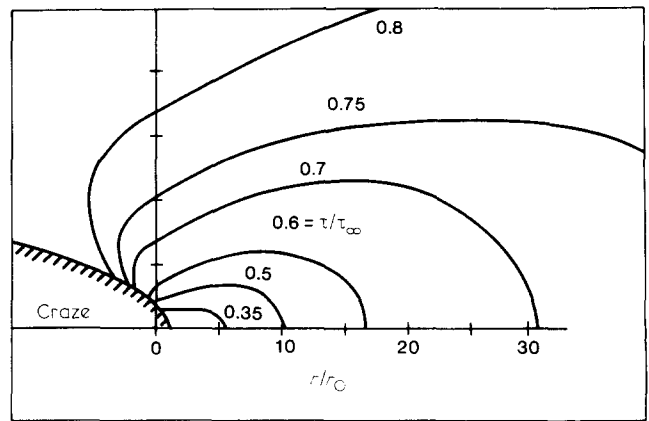


Figure 8 Contour lines of constant maximum shear stress, τ/τ_∞ , at craze tip for a uniaxial load directed parallel to the craze plane, $\gamma = 90^\circ$

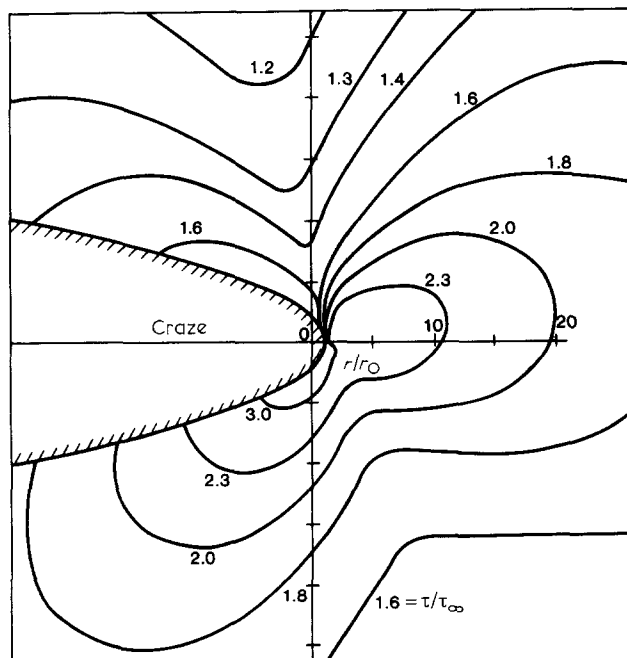


Figure 6 Contour lines of constant maximum shear stress, τ/τ_∞ , at craze tip for a uniaxial load directed 45° from the craze plane normal, $\gamma = 45^\circ$

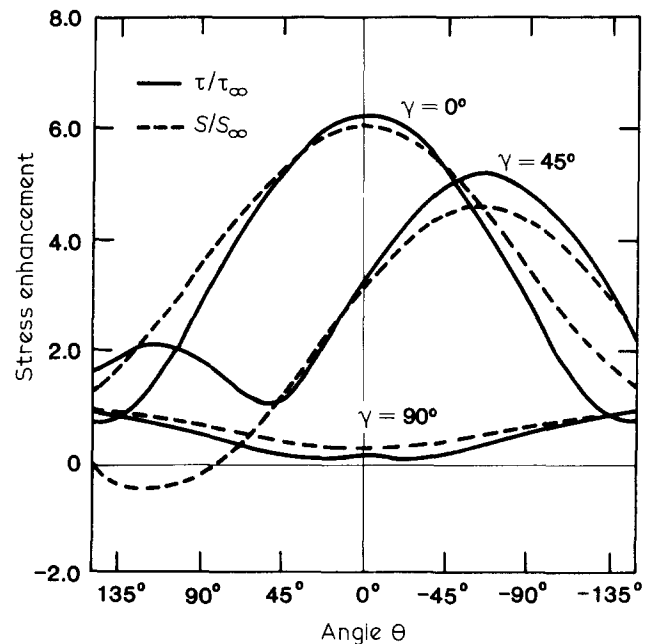


Figure 9 Variation of stresses S/S_∞ and τ/τ_∞ around the craze boundary for $\gamma = 0^\circ, 45^\circ, 90^\circ$

Table 1 Maximum stress and strain enhancements at craze tip

γ	θ_0	$(\sigma_{xx} + \sigma_{yy})$		σ_{max}	ϵ_{max}
		σ_0	τ/τ_∞	σ_0	ϵ_{max}^∞
0°	0	6.00	6.17	6.08	6.13
10°	-18.0°	5.95	6.16	6.06	6.11
20°	-34.3°	5.78	6.10	5.94	6.02
30°	-48.2°	5.45	5.89	5.67	5.79
40°	-59.9°	4.93	5.46	5.20	5.34
45°	-65.2°	4.60	5.16	4.88	5.03
50°	-70.2°	4.22	4.79	4.50	4.66
60°	-80.2°	3.36	3.89	3.62	3.77
70°	-91.5°	2.44	2.83	2.64	2.74
80°	-110.1°	1.55	1.73	1.64	1.69
90°	$\pm 180^\circ$	1.00	1.00	1.00	1.00

may influence the growth of crazes in polymers and shows the effect of the direction of applied uniaxial stress γ on these variables. These all maximize at the same point on the craze boundary as defined by the angle θ_0 . For this example there is not much difference in enhancement for any of these variables for a given direction of applied stress.

These results show that the induced stresses and strains in the bulk polymer around the tip of the craze become skewed with the angle γ such that the craze growth tends toward a direction normal to the direction of applied stress. This is consistent with the observations of Klemperer²³ who first noted that the areal growth of crazes occurs in planes normal to the direction of maximum tensile stress in isotropic polymers, and with the recent results of King and Kramer²² who show how a growing craze turns to follow the direction of maximum tensile strain in biaxially loaded specimens of polystyrene. For a uniaxial stress having direction parallel to the craze plane ($\gamma = 90^\circ$), the stresses and strains in the bulk polymer at the craze tip become very small, the maximum values then occurring near the middle of the craze with no enhancement. Thus loading parallel to the craze plane has no tendency to propagate the craze, an effect also observed by King and Kramer²².

Since the stress and strain enhancements at the craze tip are independent of the geometry of the craze for thin crazes, and in particular this enhancement is independent of craze length, these results indicate that craze growth will also be independent of craze length. A constant rate of craze growth over relatively large ranges of craze size has been experimentally observed in polystyrene at room temperature by Sauer and Hsiao²⁴.

DISCUSSION

In this analysis of the stress and displacement fields around a craze tip, the bulk polymer has been modelled as a linear isotropic elastic continuum and the craze has been modelled as a transversely isotropic elastic inclusion of very thin elliptical shape. While the elastic constants of the bulk polymer and craze are understood to be temperature dependent, this is not explicitly represented and all mechanical processes are assumed to occur at constant temperature. Viscoelastic, plastic, and rate effects are not considered. For uniform stress conditions applied in the far field, the craze region is in a state of uniform stress. Stresses in the bulk polymer exhibit their maximum values at the craze interface, and these maximum values

depend only on the material properties of the craze and bulk polymer and on the externally applied loads. In particular, the stress enhancement at the craze boundary is independent of craze length, craze thickness, radius of curvature of the craze tip or any other geometrical parameter associated with the craze. This implies that craze growth rate will be constant for any constant loading which is sufficient to initiate craze growth. Sauer and Hsiao²⁴ found this to be true for polystyrene at room temperature for craze growth beyond some initial length where they observed that the growth rate at constant load remained unchanged over large increases in craze size. Eventually, however, the effects of boundaries of a finite specimen will alter the stress field and craze growth rates can be expected to change as the craze approaches a boundary of the bulk polymer. Observations of very slow craze growth under conditions of low-stress creep²⁵ indicate a craze growth rate that slows significantly with time. This effect may be due to long time viscoelastic relaxation or hardening within the craze or bulk polymer.

This analysis predicts that the shape of the craze at the tip will be blunted rather than cusped as required by analysis which model the craze as a crack. While blunting is consistent with some observations of craze tip profiles², other observations, particularly for crazes growing at tips of cracks, indicate a cusp shape. The presence of a long crack within the craze may substantially alter the stress and displacement fields at the craze tip. The opening crack will tend to spread the craze apart which may give the appearance of a cusp while remaining blunted on a smaller scale at the craze tip. The possible effects of a crack within the craze on the stress field around the craze tip is not considered in this analysis.

A second interesting result of this stress enhancement independence on craze length relates to the establishment of a criterion for craze growth. Since the stress and strain enhancement for a given polymer-craze system depends only on the externally applied loads, craze growth criteria based on these applied loads and not on conditions existing at the craze tip would appear to be completely justified. Also, the fact that it is quite possible that all of the mechanical effects generally considered as candidates for inducing craze growth maximize at the same point on the craze boundary and with roughly the same enhancement may effectively mask the actual physical conditions required for craze growth. Based on these results, it comes as no surprise that a definitive criterion for craze growth in glassy polymers has yet to be established. But this may only represent a limitation of the elastic analysis; the highly localized stress and strain enhancements at the craze tip may be of considerably more importance under conditions where viscoelastic, plastic, or other dissipative effects are operating in the bulk polymer.

REFERENCES

- 1 Rabinowitz, S. and Beardmore, P. *Critical Reviews in Macromolecular Science*, 1, E. Baer, ed., CRC Press, Cleveland, OH (1972), p 1
- 2 Kambour, R. P. *J. Polym. Sci., D* 1973, 7, 1
- 3 Kausch, H. H. *Polymer Fracture*, Springer-Verlag, New York, 1978
- 4 Knauss, W. G. 'The Mechanics of Fracture', F. Erdogan, Ed., AMD-19, ASME, 1976, p 69
- 5 Kramer, E. J. *Developments in Polymer Fracture—1*, E. H. Andrews, Ed., Applied Science Publishers, London, 1979, p 55

- | | |
|--|--|
| <p>6 Andrews, E. H. and Reed, P. E. <i>Advances in Polymer Science</i>—
27, Springer-Verlag, Berlin, 1978, p 1</p> <p>7 Sternstein, S. S. and Ongchin, L. <i>Polymer Preprints, Am. Chem. Soc., Div. Polymer Chem.</i> 1969, 10, 2, 1117</p> <p>8 Sternstein, S. S. and Myers, F. A. <i>J. Macromol. Sci.-Phys.</i> 1973, B8, 557</p> <p>9 Oxborough, R. J. and Bowden, P. B. <i>Phil. Mag.</i> 1973, 28, 3, 547</p> <p>10 Wang, T. T., Matsuo, M. and Kwei, T. K. <i>J. Appl. Phys.</i> 1971, 42, 4188</p> <p>11 Marshall, G. P., Culver, L. E. and Williams, J. G. <i>Proc. Roy. Soc. London</i> 1970, A319, 165</p> <p>12 Andrews, E. H. and Bevan, L. <i>Polymer</i> 1972, 13, 7, 337</p> <p>13 Gent, A. N. <i>J. Mater. Sci.</i> 1970, 5, 11, 925</p> <p>14 Knight, A. C. <i>J. Polym. Sci.—A</i> 1965, 3, 1845</p> <p>15 Chen, W. T. <i>Quart. J. Mech. Appl. Math.</i> 1967, 20, 307</p> <p>16 Yang, H. C. and Chou, Y. T. <i>J. Appl. Mech., Trans. ASME</i> 1976, 43, 424</p> | <p>17 Muskhelishvili, N. I. <i>Some Basic Problems of the Mathematical Theory of Elasticity</i>, 3rd Edition, Noordhoff, Groningen, 1953</p> <p>18 Eubanks, R. A. and Sternberg, E. <i>J. Rat. Mech. and Anal.</i> 1954, 3, 89</p> <p>19 Voigt, W. <i>Rapports présentés au Congrès International de Physique</i> 1, Paris, 1900</p> <p>20 Love, A. E. H. <i>A Treatise on the Mathematical Theory of Elasticity</i>, 4th Edition, Dover Publications, New York, 1944, p 157</p> <p>21 Newman, S. B. and Wolock, I. <i>J. Res. Natl. Bur. Stds.</i> 1957, 58, 6, 339</p> <p>22 King, P. S. and Kramer, E. J. <i>J. Mat. Sci.</i> 1981, 16, 1843</p> <p>23 Klemperer, W. B. <i>Theodore von Karman Anniversary Volume, Applied Mech.</i> 1941, p 328</p> <p>24 Sauer, J. A. and Hsiao, C. C. <i>Trans. ASME</i> 1953, 75, 895</p> <p>25 Verheulpen-Heymans, N. and Bauwens, J. C. <i>J. Mater. Sci.</i> 1976, 11, 1</p> |
|--|--|